Entanglement and area laws in weakly correlated Gaussian states

J. M. Matera, R. Rossignoli, and N. Canosa

Departamento de Física–IFLP, Facultad de Ciencias Exactas, Universidad Nacional de La Plata, Casilla de Correo 67, La Plata (1900), Argentina

(Received 2 November 2012; published 26 December 2012)

We examine the evaluation of entanglement measures in weakly correlated Gaussian states. It is shown that they can be expressed in terms of the singular values of a particular block of the generalized contraction matrix. This result enables us to obtain in a simple way asymptotic expressions and related area laws for the entanglement entropy of bipartitions in pure states, as well as for the logarithmic negativity associated with bipartitions and also with pairs of arbitrary subsystems. As illustration, we consider different types of contiguous and noncontiguous blocks in two-dimensional lattices. Exact asymptotic expressions are provided for both first-neighbor and full-range couplings, which lead in the first case to area laws depending on the orientation and separation of the blocks.

DOI: 10.1103/PhysRevA.86.062324 PACS number(s): 03.67.Mn, 03.65.Ud, 05.30.Jp

I. INTRODUCTION

Entanglement is a valuable resource that plays a key role in quantum information processing and transmission based on qubits [1–4] or on continuous-variable systems [5]. It has also provided new insights into the role of quantum correlations in the critical behavior of many-body quantum systems [6–10]. Nonetheless, the evaluation of genuine quantum correlations for a given state of a many-body system is in general a difficult task. On the one hand, rigorous computable entanglement measures exist just for pure states, where the entanglement entropy, i.e., the entropy of the reduced state of a subsystem, provides the basic measure of bipartite entanglement [11]. In the case of mixed states, rigorous measures like the entanglement of formation [12], which is the convex-roof extension of the previous measure [13], involve a minimization over a very high-dimensional space of parameters and are therefore not directly computable. This has turned attention to the negativity [14], or equivalently the logarithmic negativity [14,15], which quantifies the violation of the positive-partial-transpose separability criterion by entangled states and is a bipartite entanglement monotone [14], computable in principle for any bipartition in any pure or mixed state. Nevertheless, the accurate evaluation of these quantities demands a deep knowledge of the many-body state, which requires in general an amount of information that increases exponentially with the system size. This fact limits the possibility of closed evaluations to states characterized by a manageable number of parameters [9].

Prime examples of such states are the *Gaussian states,* i.e., ground or thermal states of stable gapped Hamiltonians quadratic in boson operators, or equivalently generalized coordinates and momenta [5,16,17]. For such states, of crucial importance for continuous-variable quantum information [5], the entanglement entropy of bipartitions of pure states and the negativity between arbitrary subsystems in pure or mixed states can be evaluated in terms of the elements of the covariance matrix [18–22], i.e., of the generalized contraction matrix of pairs of boson operators [23,24]. However, even in this scenario, the extraction of analytical expressions for these quantities for arbitrary subsystems is in general not straightforward [18,19,25].

The aim of this work is to discuss the evaluation of the previous measures in weakly correlated Gaussian states, such as typical ground states of gapped Hamiltonians, which can be characterized by excitations over a product state. Gaussian states are usually described in terms of the phase-space formalism [5], which allows their entanglement properties to be connected with correlations in phase space. Here we will consider a different approach, based on the Fock representation, which provides an equivalent yet in many cases clearer way to evaluate and represent entanglement measures [24]. We will show that the entanglement entropy and negativity can be expressed in terms of the singular values of sub-blocks of basic contraction matrices, which can be evaluated analytically in the perturbative limit for some typical couplings. The formalism also allows the straightforward derivation of area laws [10,19,26–28] for these quantities. The emergent area laws for the entanglement entropy and negativity are different, i.e., they depend on distinct measures of the boundary size, and are affected by the orientation and separation of the subsystems. Let us also remark that the ground state of weakly interacting spin systems can also be described by Gaussian states through different approximate bosonization techniques [23,24,29], entailing that the scope of the present scheme is quite general.

The formalism is described in Sec. II, while Sec. III considers its application to specific systems, essentially ground states of two-dimensional lattices with short-range couplings, although the full-range case is also considered. The present scheme allows us to easily obtain exact analytical asymptotic expressions for the entanglement entropy and logarithmic negativity of different types of bipartitions and block pairs, both contiguous and separated, which will be compared with exact numerical results. They clearly show the emergence of precise area laws. Conclusions are finally drawn in Sec. IV. We also include appendixes containing the details of the perturbative expansion for the symplectic eigenvalue problem and the evaluation of singular values.

II. FORMALISM

A. Entanglement entropy and negativity in Gaussian states

The class of Gaussian states in a bosonic system can be defined as those states of the form

$$\rho = \frac{1}{\mathrm{Tr}\exp(-\beta H)} T(\alpha)\exp(-\beta H)T^{\dagger}(\alpha), \qquad (1)$$

where H is a positive definite quadratic form on the boson operators b_i and $b_i^\dagger$ ($[b_i,b_j^\dagger]=\delta_{ij}$, $[b_i,b_j]=0$),

$$\begin{aligned} H &= \sum_{i,j}(\lambda_i\delta_{ij}-\Delta_{ij}^+)\left(b_i^\dagger b_j+\frac{1}{2}\delta_{ij}\right)-\frac{1}{2}(\Delta_{ij}^- b_i b_j+\bar{\Delta}_{ij}^- b_j^\dagger b_i^\dagger) \\ &= \frac{1}{2}\mathcal{Z}^\dagger\mathcal{H}\mathcal{Z}\,, \\ \mathcal{H} &= \begin{pmatrix} \Lambda-\Delta^+ & -\Delta^- \\ -\bar{\Delta}^- & \Lambda-\bar{\Delta}^+ \end{pmatrix}, \end{aligned} \tag{2}$$

with $\mathcal{Z}=\binom{b}{b^\dagger}$, and $T(\alpha)=\prod_i \exp(\bar{\alpha}_i b_i-\alpha_i b_i^\dagger)$ is a displacement operator [$T(\alpha)b_i T^\dagger(\alpha)=b_i+\alpha_i$]. In (2), Λ is the diagonal matrix of local bare energies λ_i and $\Delta_{ij}^\pm$ are the coupling strengths between pairs of different bosons ($\Delta_{ij}^+=\bar{\Delta}_{ji}^+$, $\Delta_{ij}^-=\Delta_{ji}^-$). In the pure-state limit $\beta\to\infty$ and $\rho\to T(\alpha)|0\rangle\langle 0|T^\dagger(\alpha)$, with $|0\rangle$ the ground state of H. The displacements α_i can be taken into account by local shifts $b_i\to b_i-\alpha_i$, so that in what follows we will set $\alpha_i=0$, such that $\langle b_i\rangle_\rho\equiv \mathrm{Tr}\rho b_i=0$, $\forall i$.

The key property of these states is that by means of Wick's theorem [23] the expectation value of any bosonic operator (and hence ρ) is fully determined by the displacements α_i and the generalized contraction matrix [23,24]

$$\begin{aligned} \mathcal{D} &= \langle\mathcal{Z}\mathcal{Z}^\dagger\rangle-\mathcal{M}=\begin{pmatrix} F^+ & F^- \\ \bar{F}^- & \mathbf{1}+\bar{F}^+ \end{pmatrix}, \\ F_{ij}^+ &= \langle b_j^\dagger b_i\rangle_\rho, \quad F_{ij}^- = \langle b_i b_j\rangle_\rho, \end{aligned} \tag{3}$$

where $\mathcal{M}=\mathcal{Z}\mathcal{Z}^\dagger-[(\mathcal{Z}^\dagger)^t\mathcal{Z}^t]^t=\left(\begin{smallmatrix}\mathbf{1} & 0\\ 0 & -\mathbf{1}\end{smallmatrix}\right)$ is the *symplectic metric* and $F_{ij}^+=\bar{F}_{ji}^+$, $F_{ij}^-=F_{ji}^-$.

We may diagonalize $\mathcal{D}$ or $\mathcal{H}$ by means of a symplectic transformation $\mathcal{W}$ satisfying $\mathcal{W}^\dagger\mathcal{M}\mathcal{W}=\mathcal{M}$, corresponding to a Bogoliubov transformation $\mathcal{Z}=\mathcal{W}\mathcal{Z}'$ to boson operators $\mathcal{Z}'=\binom{b'}{b'^\dagger}$, such that $\mathcal{D}=\mathcal{W}\mathcal{D}'\mathcal{W}^\dagger$, with $\mathcal{D}'$ diagonal ($F'^+_{\alpha\alpha'}=f_\alpha\delta_{\alpha\alpha'}$, $F'^-=0$). This leads to the standard diagonalization of the matrix $\mathcal{D}\mathcal{M}$ (as $\mathcal{W}\mathcal{D}\mathcal{M}\mathcal{W}^{-1}=\mathcal{D}'\mathcal{M}$). The matrix $\mathcal{W}$ can be written in block form as

$$\mathcal{W}=\begin{pmatrix} U & V \\ \bar{V} & \bar{U} \end{pmatrix}, \tag{4}$$

where U and V should satisfy

$$U^\dagger U-V^t\bar{V}=\mathbf{1}=UU^\dagger-VV^\dagger, \tag{5a}$$

$$U^\dagger V-V^t\bar{U}=0=UV^t-VU^t. \tag{5b}$$

The blocks $F^\pm$ of the contraction matrix acquire then a simple form in terms of U, V, and the diagonal block F'^+:

$$F^-=VU^t+VF'^+U^t+UF'^+V^t, \tag{6a}$$

$$F^+=VV^\dagger+VF'^+V^\dagger+UF'^+U^\dagger. \tag{6b}$$

For a *pure state*, $F'^+=0$ and Eqs. (6) lead to $F^-=VU^t$ and $F^+=VV^\dagger$, implying

$$F^-\bar{F}^-=F^++F^{+2}. \tag{7}$$

For such states, the *entanglement* between any subsystem $\mathcal{A}$ and its complement $\bar{\mathcal{A}}$ can be measured through the von Neumann entropy of any of the reduced states:

$$\mathcal{E}_{\mathcal{A},\bar{\mathcal{A}}}=S(\rho_{\mathcal{A}})=S(\rho_{\bar{\mathcal{A}}}), \tag{8}$$

where $S(\rho)=-\mathrm{Tr}\rho\log_2\rho$. In a Gaussian state, the validity of Wick's theorem [23] implies that the state of any subsystem $\mathcal{A}$ is also Gaussian and hence fully characterized by the corresponding contraction matrix $\mathcal{D}_\mathcal{A}$, which is just the subblock of $\mathcal{D}$ with indices belonging to $\mathcal{A}$:

$$\mathcal{D}_\mathcal{A}=\begin{pmatrix} F_\mathcal{A}^+ & F_\mathcal{A}^- \\ \bar{F}_\mathcal{A}^- & \mathbf{1}+\bar{F}_\mathcal{A}^+ \end{pmatrix}. \tag{9}$$

The von Neumann entropy (8) can then be expressed in terms of the symplectic eigenvalues $f_\alpha^\mathcal{A}$ of $\mathcal{D}_\mathcal{A}$ as

$$S(\rho_\mathcal{A})=\sum_\alpha h\left(f_\alpha^\mathcal{A}\right), \quad h(x)=-x\log_2 x+(1+x)\log(1+x). \tag{10}$$

In the case of a mixed state or for pairs of noncomplementary subsystems $\mathcal{B},\mathcal{C}$, the subsystem entropy is no longer a measure of quantum correlations. Instead, a well-known computable entanglement monotone for such systems is the *negativity* $N_{\mathcal{B},\mathcal{C}}$ [14], which is just the sum of the negative eigenvalues of the *partial transpose* $\rho_{\mathcal{B}\mathcal{C}}^{t_\mathcal{B}}$. An associated quantity is the *logarithmic negativity*

$$\mathcal{E}_{\mathcal{B},\mathcal{C}}^\mathcal{N}=\log_2(1+2N_{\mathcal{B},\mathcal{C}})=\log_2\left\|\rho_{\mathcal{B}\mathcal{C}}^{t_\mathcal{B}}\right\|_1, \tag{11}$$

where $\|A\|_1=\mathrm{tr}\sqrt{A^\dagger A}$ denotes the *trace norm*. For a Gaussian state, $\|\rho_{\mathcal{B}\mathcal{C}}^{t_\mathcal{B}}\|_1$ can be expressed in terms of the *negative symplectic eigenvalues* $\tilde{f}_\alpha^{\mathcal{B},\mathcal{C}}$ of the contraction matrix $\tilde{\mathcal{D}}_{\mathcal{B}\mathcal{C}}$ determined by $\rho_{\mathcal{B}\mathcal{C}}^{t_\mathcal{B}}$, with blocks

$$\tilde{F}_{\mathcal{B}\mathcal{C}}^\pm=\begin{pmatrix} \bar{F}_\mathcal{B}^\pm & \bar{F}_{\mathcal{B},\mathcal{C}}^\mp \\ F_{\mathcal{C},\mathcal{B}}^\mp & F_\mathcal{C}^\pm \end{pmatrix}, \tag{12}$$

where $F_{\mathcal{B},\mathcal{C}}^\pm$ denotes the matrix of elements $F_{ij}^\pm$ with $i\in\mathcal{B}$ and $j\in\mathcal{C}$, and $F_\mathcal{B}^\pm\equiv F_{\mathcal{B},\mathcal{B}}^\pm$. Equation (11) then becomes

$$\mathcal{E}_{\mathcal{B},\mathcal{C}}^\mathcal{N}=\sum_{\tilde{f}_\alpha^{\mathcal{B},\mathcal{C}}<0} g\left(\tilde{f}_\alpha^{\mathcal{B},\mathcal{C}}\right), \quad g(x)=-\log_2(1+2x). \tag{13}$$

We notice that $\tilde{f}_\alpha^{\mathcal{B},\mathcal{C}}\geqslant -1/2$ [24]. In the case where $\mathcal{B}=\mathcal{A}$ and $\mathcal{C}=\bar{\mathcal{A}}$, Eq. (13) can be expressed in terms of the symplectic eigenvalues $f_\alpha^\mathcal{A}$ of $\mathcal{D}_\mathcal{A}$ as [24]

$$\mathcal{E}_{\mathcal{A},\bar{\mathcal{A}}}^\mathcal{N}=2\sum_\alpha\log_2\left(\sqrt{f_\alpha^\mathcal{A}}+\sqrt{1+f_\alpha^\mathcal{A}}\right), \tag{14}$$

which, like Eq. (8), is again a concave function of the $f_\alpha^\mathcal{A}$.

B. Weakly correlated pure Gaussian states

We consider now the case of weakly correlated pure Gaussian states, i.e., states in which the local symplectic eigenvalues (those corresponding to a single mode $\mathcal{A}=i$)

$$f_i=\sqrt{\left(\frac{1}{2}+F_{ii}^+\right)^2-|F_{ii}^-|^2}-\frac{1}{2} \tag{15}$$

satisfy $f_i\ll 1$, $\forall\, i$, such that each mode is weakly entangled with the rest of the system. In the local basis where $F_{ii}^-=0$ (this implies replacing $b_i\to u_i b_i-e^{i\phi}v_i b_i^\dagger$, with $u_i,v_i=\sqrt{\frac{F_{ii}^+ +1/2\pm(f_i+1/2)}{2f_i+1}}$ and ϕ the phase of F_{ii}^-), $f_i=F_{ii}^+$ and weak coupling implies, together with the positivity of $\mathcal{D}$ and F^+,

that $|F^+_{ij}| \leqslant \sqrt{f_i f_j} \ll 1$, $|F^-_{ij}|^2 \leqslant \mathrm{Min}[f_i, f_j] + f_i f_j \ll 1$, $\forall$ i, j. In this limit, Eqs. (6) and (7) then lead, neglecting terms proportional to $(F^- \bar{F}^-)^2$, to

$$F^+ \approx F^- \bar{F}^-, \tag{16}$$

which for a subsystem $\mathcal{A}$ implies

$$F^+_{\mathcal{A}} \approx F^-_{\mathcal{A}} \bar{F}^-_{\mathcal{A}} + F^-_{\mathcal{A},\bar{\mathcal{A}}} \bar{F}^-_{\bar{\mathcal{A}},\mathcal{A}}. \tag{17}$$

Using Eq. (17) and the results of Appendix A, the symplectic eigenvalues of $\mathcal{D}_{\mathcal{A}}$ will then agree at this order with the standard eigenvalues of the matrix

$$F^+_{\mathcal{A}} - F^-_{\mathcal{A}} \bar{F}^-_{\mathcal{A}} \approx F^-_{\mathcal{A},\bar{\mathcal{A}}} \bar{F}^-_{\bar{\mathcal{A}},\mathcal{A}}, \tag{18}$$

which are just the squares of the *singular values* $\sigma_\alpha^{\mathcal{A},\bar{\mathcal{A}}}$ of $F^-_{\mathcal{A},\bar{\mathcal{A}}}$ (see Appendix B). We then obtain, at this order,

$$f_\alpha^{\mathcal{A}} \approx \left(\sigma_\alpha^{\mathcal{A},\bar{\mathcal{A}}}\right)^2. \tag{19}$$

Entanglement depends at this level just on the F^- contractions between $\mathcal{A}$ and $\bar{\mathcal{A}}$. For instance, in the case of a single site i, Eq. (19) implies $f_i \approx \sigma^2_{i,\bar{i}} = \sum_{j\neq i} |F^-_{ij}|^2$. In this regime we may just set $h(x) \approx -x \log_2(x/e)$ in Eq. (10), such that the entanglement entropy becomes

$$\mathcal{E}_{\mathcal{A},\bar{\mathcal{A}}} \approx -\sum_\alpha \left(\sigma_\alpha^{\mathcal{A},\bar{\mathcal{A}}}\right)^2 \log_2\left[\left(\sigma_\alpha^{\mathcal{A},\bar{\mathcal{A}}}\right)^2/e\right]. \tag{20}$$

Considering now the negativity, in the present regime the symplectic eigenvalues of $\tilde{\mathcal{D}}_{\mathcal{BC}}$ will be given at leading order by the eigenvalues of (see Appendix A)

$$\tilde{F}^+_{\mathcal{BC}} - \tilde{F}^-_{\mathcal{BC}} \bar{\tilde{F}}^-_{\mathcal{BC}} \approx \begin{pmatrix} \bar{G}_{\mathcal{B}} & \bar{F}^-_{\mathcal{B},\mathcal{C}} \\ F^-_{\mathcal{C},\mathcal{B}} & G_{\mathcal{C}} \end{pmatrix}, \tag{21}$$

where, for $\mathcal{S} = \mathcal{B}$ or $\mathcal{C}$,

$$G_{\mathcal{S}} = F^+_{\mathcal{S}} - F^-_{\mathcal{S}} \bar{F}^-_{\mathcal{S}}. \tag{22}$$

For pure global states, Eq. (18) leads to $G_{\mathcal{S}} \approx F^-_{\mathcal{S},\bar{\mathcal{S}}} \bar{F}^-_{\bar{\mathcal{S}},\mathcal{S}}$, indicating that $\mathcal{G}_{\mathcal{S}}$ takes into account the correlations with the environment of $\mathcal{S}$. Up to first order in $F^-_{\mathcal{B},\mathcal{C}}$, we may neglect its second-order effect in $G_{\bar{\mathcal{B}}}$ and $G_{\mathcal{C}}$ in Eq. (21), such that

$$G_{\mathcal{B}} \approx F^-_{\mathcal{B},\overline{\mathcal{BC}}} \bar{F}^-_{\overline{\mathcal{BC}},\mathcal{B}}, \quad G_{\mathcal{C}} \approx F^-_{\mathcal{C},\overline{\mathcal{BC}}} \bar{F}^-_{\overline{\mathcal{BC}},\mathcal{C}} \tag{23}$$

depend just on the correlation with the environment of $\mathcal{BC}$. If the sites of $\mathcal{B}$ and $\mathcal{C}$ correlated with each other have correlations of the same order (or lower) with $\overline{\mathcal{BC}}$ (i.e., $\|F^-_{\mathcal{B},\overline{\mathcal{BC}}}\|_\infty$ and $\|F^-_{\mathcal{C},\overline{\mathcal{BC}}}\|_\infty$ of the same order as $\|F^-_{\mathcal{B},\mathcal{C}}\|_\infty$, at least for the subsets of $\mathcal{B}$ and $\mathcal{C}$ mutually correlated) we can directly neglect $G_{\mathcal{B}}$ and $G_{\mathcal{C}}$ in Eq. (21) at order $\|F^-_{\mathcal{B},\mathcal{C}}\|_\infty$. The negative symplectic eigenvalues of $\tilde{\mathcal{D}}_{\mathcal{B},\mathcal{C}}$ will then be given by minus the singular values $\sigma_\alpha^{\mathcal{B},\mathcal{C}}$ of $F^-_{\mathcal{B},\mathcal{C}}$ (see Appendix B):

$$\tilde{f}_\alpha^{\mathcal{B},\mathcal{C}} \approx -\sigma_\alpha^{\mathcal{B},\mathcal{C}}, \tag{24}$$

which depend again just on the F^- contractions between $\mathcal{B}$ and $\mathcal{C}$. For instance, this is the case of contiguous blocks in a scenario of short-range couplings, and also that where $\mathcal{C}$ is the complement of $\mathcal{B}$ ($\mathcal{C} = \bar{\mathcal{B}}$).

In the general case, however, the whole matrix (21) should be diagonalized. First-order corrections lead to

$$\tilde{f}_\alpha^{\mathcal{B},\mathcal{C}} \approx -\sigma_\alpha^{\mathcal{B},\mathcal{C}} + [(\bar{G}_{\mathcal{B}})_{\alpha\alpha} + (G_{\mathcal{C}})_{\alpha\alpha}]/2, \tag{25}$$

where $(\bar{G}_{\mathcal{B}})_{\alpha\alpha} = U^\dagger_\alpha \bar{G}_{\mathcal{B}} U_\alpha$ and $(G_{\mathcal{C}})_{\alpha\alpha} = V^\dagger_\alpha G_{\mathcal{B}} V_\alpha$ are the diagonal elements in the local basis of $\mathcal{B}$ and $\mathcal{C}$ where $(\mathcal{F}^-_{\mathcal{B},\mathcal{C}})_{\alpha\alpha'} = \sigma_\alpha^{\mathcal{B},\mathcal{C}} \delta_{\alpha\alpha'}$ (see Appendix B). As $G_{\mathcal{B}}$ and $G_{\mathcal{C}}$ are positive matrices in the approximations (22) and (23), negative eigenvalues can arise only if $(G_{\mathcal{B}})_{\alpha\alpha}$ and $(G_{\mathcal{C}})_{\alpha\alpha}$ are not much larger than $\sigma_\alpha^{\mathcal{B},\mathcal{C}}$. A sufficient condition ensuring a negative eigenvalue $\tilde{f}_\alpha^{\mathcal{B},\mathcal{C}}$ of Eq. (21) is

$$\sigma_\alpha^{\mathcal{B},\mathcal{C}} > \sqrt{(\bar{G}_{\mathcal{B}})_{\alpha\alpha}(G_{\mathcal{C}})_{\alpha\alpha}}. \tag{26}$$

In the present regime, the logarithmic negativity can be obtained by setting $g(x) \approx -2\log_2(e)x$ in Eq. (13), such that

$$\mathcal{E}^{\mathcal{N}}_{\mathcal{B},\mathcal{C}} \approx -2\log_2(e) \sum_{\tilde{f}_\alpha^{\mathcal{B},\mathcal{C}}<0} \tilde{f}_\alpha^{\mathcal{B},\mathcal{C}}, \tag{27}$$

i.e., $\mathcal{E}^{\mathcal{N}}_{\mathcal{B},\mathcal{C}} \propto \|F^-_{\mathcal{B},\mathcal{C}}\|_1$ in the approximation (24). For complementary subsystems ($\mathcal{C} = \bar{\mathcal{B}} = \bar{\mathcal{A}}$), it is verified that identity between Eqs. (14) and (27) holds at leading order in the approximation (19) [$\log_2(\sigma + \sqrt{1+\sigma^2}) \approx \log_2(e)\sigma$].

C. Ground-state correlation matrix in the weakly interacting case

A particular case of the previous results arises when we deal with the ground state of a Hamiltonian of the form (2). For weak couplings $\Delta^\pm \ll \Lambda$, the diagonalizing symplectic transformation $\mathcal{W}$ such that $\mathcal{W}^\dagger \mathcal{H} \mathcal{W} = \Omega \oplus \Omega$, with $\Omega_{\alpha\alpha'} = \delta_{\alpha\alpha'}\omega_\alpha$, can be evaluated perturbatively. At leading order (see Appendix A) the block U in Eq. (4) is a *unitary* matrix that diagonalizes $\Lambda - \Delta^+$, while

$$V_{i\beta} \approx \sum_\alpha U_{i\alpha} \frac{(U^\dagger \Delta^- \overline{U})_{\alpha\beta}}{\omega_\alpha + \omega_\beta}. \tag{28}$$

Note that, in contrast with the conventional perturbation theory, a possible degeneracy in the local energies λ_k will not spoil this result if the system is stable ($\omega_\alpha > 0$, $\forall$ α). Notice, however, that U can depart considerably from the identity if the λ_k are degenerate.

If all local bare energies are nearly equal ($|\lambda_k - \lambda_j| \ll \lambda_k + \lambda_j \approx 2\lambda$), and if energy corrections arising from Δ^+ are neglected ($\omega_\alpha \approx \lambda$), Eq. (28) reduces to $V \approx \frac{1}{2\lambda}\Delta^- \bar{U}$. In such a case, Eq. (6) leads to

$$F^- \approx \frac{\Delta^-}{2\lambda}, \tag{29}$$

with F^+ given by Eq. (16). In this regime, correlations are hence proportional to the pairing couplings Δ^-, decreasing as λ^{-1} for increasing local energies. It is noteworthy that the strength of the hopping interaction Δ^+ does not affect the ground-state correlations at this order. When nondegenerate, it just affects $F^\pm$ dressing the bare pairing interactions.

In the same way, for a common local bare energy λ, inclusion of second-order terms in the couplings leads to

$$F^- \approx \frac{\Delta^-}{2\lambda} + \frac{\Delta^+\Delta^- + \Delta^-\bar{\Delta}^+}{4\lambda^2}. \tag{30}$$

This expression is useful in the present scheme when the first-order term vanishes (modes i, j are unconnected by Δ^-). As the counterterms $G_{\mathcal{B}}$ and $G_{\mathcal{C}}$ in Eq. (25) will be of second

order in F^- [Eq. (23)], subsystems unconnected by Δ^- but connected at second order through Eq. (30) may exhibit an $O(\Delta/\lambda)^2$ nonzero negativity if Eq. (26) holds.

D. Area laws

The formulation of the area law for systems with local interactions starts with the definition of a suitable measure for the size of the boundary $\partial\mathcal{A}$ of the subsystem $\mathcal{A}$ [10,19,25]. An example of such a measure is given by the number of pairs of first-neighbor modes, with one mode belonging to $\mathcal{A}$ and the other to $\bar{\mathcal{A}}$. If we define the matrix M with entries $M_{ij} = 1$ if modes i and j are first neighbors and 0 otherwise, that measure can be written as

$$|\partial\mathcal{A}|_2 = \sum_{i\in\mathcal{A}} n_i^{\bar{\mathcal{A}}} = \mathrm{Tr}[M_{\mathcal{A},\bar{\mathcal{A}}} M_{\bar{\mathcal{A}},\mathcal{A}}] = \|M_{\mathcal{A},\bar{\mathcal{A}}}\|_2^2, \tag{31}$$

where $n_i^{\bar{\mathcal{A}}} = (M_{\mathcal{A},\bar{\mathcal{A}}} M_{\bar{\mathcal{A}},\mathcal{A}})_{ii}$ is the number of first neighbors of mode i in $\bar{\mathcal{A}}$. For the ground state of a gapped bosonic system with constant and *isotropic* first-neighbor interactions $\Delta_{ij}^{\pm} = \frac{\Delta^{\pm}}{2} M_{ij}$, Eq. (29) implies $F_{\bar{\mathcal{A}}\mathcal{A}}^- \approx \frac{\Delta^-}{4\lambda} M_{\bar{\mathcal{A}}\mathcal{A}}$ and Eqs. (19) and (20) lead then to

$$\mathcal{E}_{\mathcal{A},\bar{\mathcal{A}}} \propto |\partial\mathcal{A}|_2, \tag{32}$$

at leading order in Δ^-/λ, which coincides exactly with the result in Ref. [19] for noncritical harmonic systems.

The logarithmic negativity presents, however, a slightly different behavior: for contiguous subsystems, the same procedure and Eqs. (24)–(27) lead to

$$\mathcal{E}^{\mathcal{N}}_{\mathcal{A},\bar{\mathcal{A}}} \propto |\partial\mathcal{A}|_1, \tag{33}$$

where the boundary measure is now

$$|\partial\mathcal{A}|_1 = \mathrm{Tr}\sqrt{M_{\mathcal{A},\bar{\mathcal{A}}} M_{\bar{\mathcal{A}},\mathcal{A}}} = \|M_{\mathcal{A},\bar{\mathcal{A}}}\|_1 = \sum_\alpha \tilde{\sigma}_\alpha^{\mathcal{A},\bar{\mathcal{A}}}, \tag{34}$$

with $\tilde{\sigma}_\alpha^{\mathcal{A},\bar{\mathcal{A}}}$ the singular values of the matrix $M_{\mathcal{A},\bar{\mathcal{A}}}$ [in comparison, $\|M_{\mathcal{A},\bar{\mathcal{A}}}\|_2^2 = \sum_\alpha (\tilde{\sigma}_\alpha^{\mathcal{A},\bar{\mathcal{A}}})^2$]. If each site in $\bar{\mathcal{A}}$ has at most one neighbor in $\mathcal{A}$ (the opposite may not hold), the rows of $M_{\mathcal{A},\bar{\mathcal{A}}}$ will be orthogonal and the singular values will be $\tilde{\sigma}_i^{\mathcal{A},\bar{\mathcal{A}}} = \sqrt{n_i^{\bar{\mathcal{A}}}}$, leading to

$$|\partial\mathcal{A}|_1 = \sum_{i\in\mathcal{A}} \sqrt{(M_{\mathcal{A},\bar{\mathcal{A}}} M_{\bar{\mathcal{A}},\mathcal{A}})_{ii}} = \sum_{i\in\mathcal{A}} \sqrt{n_i^{\bar{\mathcal{A}}}}, \tag{35}$$

which will differ from Eq. (31) if $n_i^{\bar{\mathcal{A}}} > 1$. In general, Eq. (35) may provide a rough approximation to the area (34). Interestingly, in an isotropic hypercubic lattice in d dimensions, the approximation (35) is just proportional to the Euclidean area for large planar surfaces, both parallel and tilted (with an angle of $\pi/4$ with respect to the principal axes of the lattice), which is not true in the tilted case for neither $|\partial\mathcal{A}|_2$ nor $|\partial\mathcal{A}|_1$ (see the next section).

In general, for two contiguous subsystems $\mathcal{B}$ and $\mathcal{C}$, the previous expressions generalize to

$$\mathcal{E}^{\mathcal{N}}_{\mathcal{B},\mathcal{C}} \propto |\partial\mathcal{B} \cap \partial\mathcal{C}|_1, \tag{36}$$

at leading order in λ, where

$$|\partial\mathcal{B} \cap \partial\mathcal{C}|_1 = \|M_{\mathcal{B},\mathcal{C}}\|_1 = \sum_\alpha \tilde{\sigma}_\alpha^{\mathcal{B},\mathcal{C}} \tag{37}$$

is a measure of the contacting area between $\mathcal{B}$ and $\mathcal{C}$. Again, if each mode in $\mathcal{C}$ is linked with at most one mode in $\mathcal{B}$, $\tilde{\sigma}_i^{\mathcal{B},\mathcal{C}} = \sqrt{n_i^{\mathcal{C}}}$, where $n_i^{\mathcal{C}} = (M_{\mathcal{B},\mathcal{C}} M_{\mathcal{C},\mathcal{B}})_{ii}$ is the number of first neighbors of i in $\mathcal{C}$.

Previous geometriclike expressions can of course be also applied to *a general constant coupling* $\Delta_{ij}^- = \frac{1}{2}\Delta^- M_{ij}$, where $M_{ij} = 1$ if pairs i,j are linked by the coupling and 0 otherwise, leading to effective areas $|\partial\mathcal{A}|_1 = \|M_{\mathcal{A},\bar{\mathcal{A}}}\|_1$ and $|\partial\mathcal{A}|_2 = \|M_{\mathcal{A},\bar{\mathcal{A}}}\|_2^2$. On the other hand, they cannot be directly applied to higher-order effects, like those depending on Eq. (30), as discussed in the next section.

III. EXAMPLES AND ASYMPTOTIC EXPRESSIONS

We will now use the present formalism to obtain analytic asymptotic expressions for $\mathcal{E}_{\mathcal{A},\bar{\mathcal{A}}}$ and $\mathcal{E}^{\mathcal{N}}_{\mathcal{B},\bar{\mathcal{C}}}$ for typical subsystems $\mathcal{A}$, $\mathcal{B}$, and $\mathcal{C}$ of a two-dimensional lattice, which will be compared with the exact numerical results and the estimations (32)–(36). We first consider the ground state of a bosonic square lattice with attractive first-neighbor couplings

$$\Delta_{\boldsymbol{ij}}^{\pm} = \tfrac{1}{2} \sum_{\mu=x,y} \Delta_\mu^{\pm} \left(\delta_{\boldsymbol{i},\boldsymbol{j}+\boldsymbol{u}_\mu} + \delta_{\boldsymbol{i},\boldsymbol{j}-\boldsymbol{u}_\mu}\right)$$

where $\boldsymbol{u}_\mu$ denotes the unit vector along the μ axis. We have considered in Figs. 1–6 the isotropic case $\Delta_x^{\pm} = \Delta_y^{\pm} = \Delta^{\pm}$, with $\Delta^-/\Delta^+ = 2/3$, and a uniform single-mode energy $\lambda_i = \lambda$. Away from the critical point $\lambda = \lambda_c$ (where, for fixed $\Delta^{\pm}$, the lowest energy ω_α vanishes), the system is gapped and a finite correlation length $\xi < \infty$ is expected. Approximately, $\lambda_c \approx 2(\Delta^+ + |\Delta^-|)$ (an exact result for the cyclic case [24]).

A. Entanglement between complementary subsystems

We first consider the four global $(\mathcal{A},\bar{\mathcal{A}})$ bipartitions depicted in Fig. 1. Equations (19), (24), and (29) lead to analytic

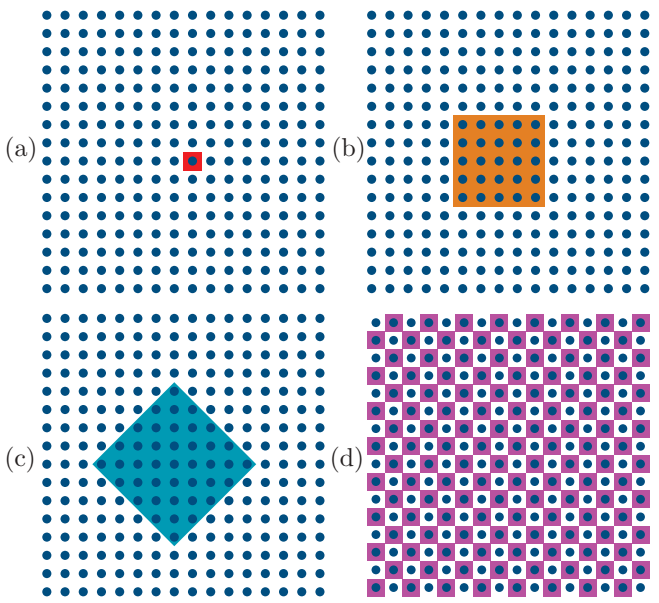

FIG. 1. (Color online) The complementary partitions considered in Eqs. (42). (a) Single site, (b) square block parallel to the principal lattice axes, (c) tilted square block, and (d) checkerboard.

asymptotic expressions for the corresponding singular values $\sigma_\alpha^{\mathcal{A},\bar{\mathcal{A}}}$. At lowest order, their number is just the number of sites at the border. Defining the basic single-link singular values

$$\sigma_\mu = |\Delta_\mu^-|/(4\lambda), \quad \mu = x,y,$$

in the case of a single site [Fig. 1(a)] we obtain

$$\sigma_{i,\bar{i}} \approx \sqrt{2\left(\sigma_x^2+\sigma_y^2\right)}. \tag{38}$$

In the rectangular $n_x \times n_y$ block of Fig. 1(b) (parallel to the principal axes), there are three different singular values, corresponding to the horizontal and vertical sides and the four corners, given below with their multiplicities:

$$\left(\sigma_\alpha^{\mathcal{A},\bar{\mathcal{A}}}\right)^2 \approx \begin{cases} \sigma_y, & 2(n_x-2), \\ \sigma_x, & 2(n_y-2), \\ \sqrt{\sigma_x^2+\sigma_y^2}, & 4. \end{cases} \tag{39}$$

In the $n \times n$ square block of Fig. 1(c) tilted at 45° with respect to the principal axes, we obtain, by means of a discrete Fourier transform and neglecting corner effects [see Eq. (C3)],

$$\sigma_k^{\mathcal{A},\bar{\mathcal{A}}} \approx \sqrt{\sigma_x^2+\sigma_y^2+2\sigma_x\sigma_y\cos\frac{2\pi k}{m}}, \tag{40}$$

where $k = 1,\ldots,m$ and $m = 4n-4$ is the number of sites at the border. Corner effects will affect essentially just four of these eigenvalues with $O(1)$ corrections.

Finally, in the checkerboard partition of Fig. 1(d), an exact analytic expression for the $n_x n_y/2$ singular values is available in the cyclic case, again by means of a discrete Fourier transform [see Eq. (41) in Ref. [29]]:

$$\sigma_{\boldsymbol{k}}^{\mathcal{A},\bar{\mathcal{A}}} \approx 2\left|\sum_{\mu=x,y}\sigma_\mu\cos\frac{2\pi k_\mu}{n_\mu}\right|, \tag{41}$$

where $\boldsymbol{k} = (k_x,k_y)$ with $k_x = 1,\ldots,n_x$, $k_y = 1,\ldots,n_y/2$.

These expressions, together with Eqs. (19), (20), (24), and (27), allow the asymptotic values of the entanglement entropy and negativity of the present bipartitions for large λ and n to be easily obtained. For instance, in the isotropic case $\Delta_\mu^\pm = \Delta^\pm$ considered in the figures, setting $\sigma = \sigma_\mu$ and neglecting corner and border effects (which just add terms of relative order n^{-1}), we obtain

$$\mathcal{E}_{i,\bar{i}}^a \approx -4\sigma^2\log_2\frac{4\sigma^2}{e}, \tag{42a}$$

$$\mathcal{E}_{\mathcal{A},\bar{\mathcal{A}}}^b \approx -4n\sigma^2\log_2\frac{\sigma^2}{e}, \tag{42b}$$

$$\mathcal{E}_{\mathcal{A},\bar{\mathcal{A}}}^c \approx -8n\sigma^2\log_2\sigma^2 = -(4n)2\sigma^2\log_2\left(\frac{e}{2}\frac{2\sigma^2}{e}\right), \tag{42c}$$

$$\mathcal{E}_{\mathcal{A},\bar{\mathcal{A}}}^d \approx -2n^2\log_2(\sigma^2 e) = -\left(\frac{n^2}{2}\right)4\sigma^2\log_2\left(\frac{e^2}{4}\frac{4\sigma^2}{e}\right) \tag{42d}$$

for the entanglement entropy of the single mode, the parallel and tilted $n \times n$ square blocks, and the $n \times n$ checkerboard of Fig. 1. We have replaced sums over k in Eqs. (42c) and (42d) by integrals $[\sum_{k=1}^n f(\frac{2\pi k}{n}) \approx \frac{n}{2\pi}\int_0^{2\pi} f(u)du]$. Note that in the checkerboard case the entanglement entropy scales with the "volume" n^2 of $\mathcal{A}$ rather than the "area" n, since all links are broken by the partition (maximally entangled bipartition [29]).

The corresponding values of the scaled logarithmic negativity $\tilde{\mathcal{E}}_{\mathcal{A},\bar{\mathcal{A}}}^{\mathcal{N}} = \mathcal{E}_{\mathcal{A},\bar{\mathcal{A}}}^{\mathcal{N}}/[2\log_2(e)]$ are

$$\tilde{\mathcal{E}}_{i,\bar{i}}^{\mathcal{N}\,a} \approx 2\sigma = \sqrt{4}\sigma, \tag{43a}$$

$$\tilde{\mathcal{E}}_{\mathcal{A},\bar{\mathcal{A}}}^{\mathcal{N}\,b} \approx 4n\sigma, \tag{43b}$$

$$\tilde{\mathcal{E}}_{\mathcal{A},\bar{\mathcal{A}}}^{\mathcal{N}\,c} \approx \frac{16}{\pi}n\sigma = (4n)\sqrt{2}\frac{2\sqrt{2}}{\pi}\sigma, \tag{43c}$$

$$\tilde{\mathcal{E}}_{\mathcal{A},\bar{\mathcal{A}}}^{\mathcal{N}\,d} \approx \frac{8n^2}{\pi^2}\sigma = \left(\frac{n^2}{2}\right)\sqrt{4}\left(\frac{2\sqrt{2}}{\pi}\right)^2\sigma\,. \tag{43d}$$

The last expressions in Eqs. (42) and (43) indicate the way to read them. They are of the form

$$\mathcal{E}_{\mathcal{A},\bar{\mathcal{A}}} \approx -Lm\,\sigma^2\,\log_2\left(\alpha^j\frac{m\sigma^2}{e}\right), \tag{44}$$

$$\tilde{\mathcal{E}}_{\mathcal{A},\bar{\mathcal{A}}}^{\mathcal{N}} \approx L\sqrt{m}\,\beta^j\sigma\,, \tag{45}$$

where L is the number of modes at the border of $\mathcal{A}$ ($L = 1,4n,4n,n^2/2$), m is the number of connections with the environment $\bar{\mathcal{A}}$ per mode at the border ($m = 4,1,2,4$), i.e., the number of links per mode broken by the partition, and α^j,β^j, with $\alpha = e/2 \approx 1.36$, $\beta = 2\sqrt{2}/\pi \approx 0.9$, are *geometric* correction factors for the tilted ($j = 1$) and checkerboard ($j = 2$) cases ($j = 0$ for the single mode and parallel square). We can easily identify from Eqs. (44) and (45) the boundary measures of Eqs. (32) and (33):

$$|\partial\mathcal{A}|_2 = Lm, \quad |\partial\mathcal{A}|_1 = L\sqrt{m}\beta^j\,. \tag{46}$$

Comparison with the exact numerical results (Fig. 2) indicate that all these asymptotic expressions are actually quite accurate already for $\lambda \gtrsim 4\lambda_c$. The scaling of $\mathcal{E}_{\mathcal{A},\bar{\mathcal{A}}}^{\mathcal{N}}$ with the area $|\partial\mathcal{A}|_1$ rather than $|\partial\mathcal{A}|_2$ is clearly verified. Moreover, this scaling is more accurate than that of the entanglement entropy $\mathcal{E}_{\mathcal{A},\bar{\mathcal{A}}}$ with $|\partial\mathcal{A}|_2$, since the latter contains in Figs. 1(c) and 1(d) an additional geometric correction $Lm\log_2(\alpha^j m)\sigma^2$ [Eq. (44)], not comprised in Eq. (32). Note also that in the case of the tilted block, $|\partial\mathcal{A}|_2 = 2L$ and $|\partial\mathcal{A}|_1 = L\sqrt{2}\beta = (4/\pi)L$ are, respectively, larger and smaller (90%) than the geometric perimeter $\sqrt{2}L$.

We may also rapidly determine with Eqs. (39), (44), and (45) the corner effects in the case of Fig. 1(b). The actual asymptotic expressions for the finite $n \times n$ parallel block are

$$\mathcal{E}_{\mathcal{A},\bar{\mathcal{A}}}^b \approx -4(n-1)\sigma^2\log_2\frac{\sigma^2}{e} - 4\sigma^2\log_2\frac{4\sigma^2}{e}, \tag{47}$$

$$\tilde{\mathcal{E}}_{\mathcal{A},\bar{\mathcal{A}}}^{\mathcal{N}\,b} \approx 4(n-1)\sigma + 4(\sqrt{2}-1)\sigma, \tag{48}$$

where the first term is proportional to the number of sites at the border, $4(n-1)$, and the second represents the positive correction arising from the four corners, reflecting their increased coupling with the environment $\bar{\mathcal{A}}$.

B. Noncomplementary subsystems

Let us now consider the noncomplementary subsystems of Fig. 3. For contiguous parallel blocks contacting at n sites,

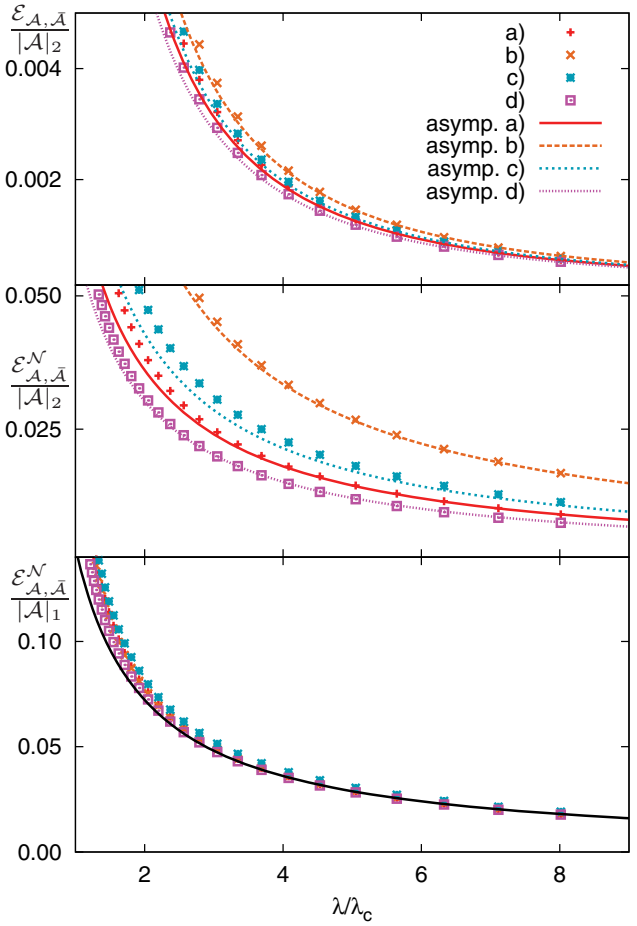

FIG. 2. (Color online) Exact and asymptotic [Eqs. (42) and (43)] results for the scaled entanglement entropy $\mathcal{E}_{\mathcal{A},\bar{\mathcal{A}}}$ (top) and logarithmic negativity $\mathcal{E}^{\mathcal{N}}_{\mathcal{A},\bar{\mathcal{A}}}$ (center and bottom) of the four bipartitions (a), (b), (c), and (d) of Fig. 1, as functions of the ratio λ/λ_c. In the top and central panels results were scaled with the boundary measure $|\partial\mathcal{A}|_2$ [$4,4n,8n,2n^2$ in (a),(b),(c),(d), according to Eqs. (31)–(46)], which is seen to provide an adequate scaling for $\mathcal{E}_{\mathcal{A},\bar{\mathcal{A}}}$ but not $\mathcal{E}^{\mathcal{N}}_{\mathcal{A},\bar{\mathcal{A}}}$. The latter scales accurately with the measure $|\partial\mathcal{A}|_1$ [$2,4n,(16/\pi)n,8n^2/\pi^2$ according to Eqs. (34)–(46)], as verified in the bottom panel. Results correspond to a 30×30 lattice with $\Delta^-/\Delta^+ = 2/3$ and 10×10 blocks in (b) and (c).

$F^-_{\mathcal{B},\mathcal{C}}$ has n identical singular values

$$\sigma_\alpha^{\mathcal{B},\mathcal{C}} = \sigma_x. \tag{49}$$

In the case of contiguous blocks with contacting surfaces tilted at 45° with respect to the principal axes, we obtain, neglecting edge effects, the same expression (40) for the $\sigma_k^{\mathcal{B},\mathcal{C}}$, with m replaced by the number of contacting sites n and $k = 1,\ldots,n$. In the isotropic case we then obtain, using Eqs. (24)–(27),

$$\tilde{\mathcal{E}}^{\mathcal{N}a}_{\mathcal{B},\bar{\mathcal{C}}} \approx n\sigma, \tag{50}$$

$$\tilde{\mathcal{E}}^{\mathcal{N}b}_{\mathcal{B},\bar{\mathcal{C}}} \approx \frac{4}{\pi}n\sigma = n\sqrt{2}\frac{2\sqrt{2}}{\pi}\sigma, \tag{51}$$

for the logarithmic negativity of parallel and tilted contiguous blocks, which are clearly of the form (45) or (33): $|\partial\mathcal{B}\cap\partial\mathcal{C}|_1 = n$ and $4n/\pi$, respectively. Tilted boundary surfaces exhibit a larger entanglement per contacting site due to the increased connectivity.

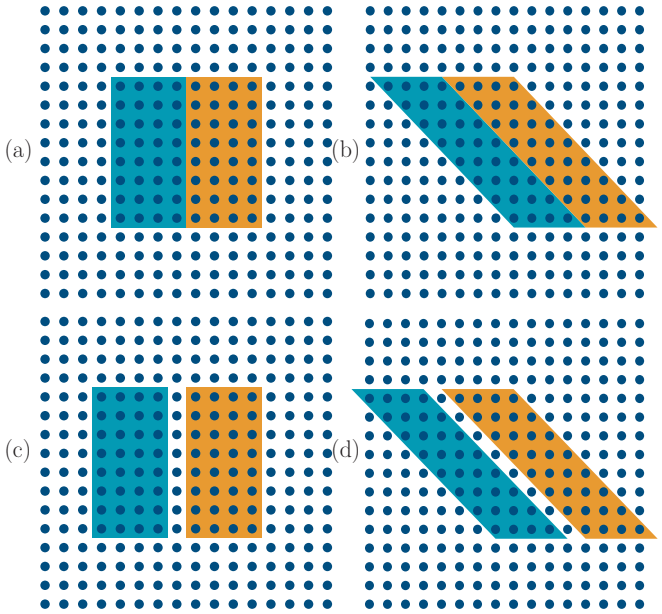

FIG. 3. (Color online) Noncomplementary subsystems: Contiguous (top) and one-site-separated (bottom) blocks, with contacting sides parallel (left) and tilted (right) with respect to the principal axes. The negativity and its size dependence are determined by both the separation and slope of the contacting boundary.

In the case of blocks separated by one site, we should use instead the full Eq. (25) with the *second-order* expression (30). For parallel blocks with n sites at separation $s = 1$, the n negative eigenvalues of the matrix (21) become, neglecting edge effects and setting $\sigma_\mu^+ = |\Delta_\mu^+|/(4\lambda)$,

$$\tilde{f}_\alpha^{\mathcal{B},\mathcal{C}} \approx -\left(2\sigma_x^+\sigma_x - \sigma_x^2\right). \tag{52}$$

For blocks separated by one site through a 45° tilted surface of n modes, a discrete Fourier transform leads, neglecting edge effects, to [see Eq. (C3)]

$$\tilde{f}_k^{\mathcal{B},\mathcal{C}} \approx -\left\{2\left[\alpha_{xy}^2 + \alpha_x^2 + \alpha_y^2 + 2\alpha_{xy}(\alpha_x+\alpha_y)\cos\frac{2\pi k}{n} + 2\alpha_x\alpha_y\cos\frac{4\pi k}{n}\right]^{1/2} - \sigma_k^2\right\}, \tag{53}$$

where $\alpha_\mu = \sigma_\mu^+\sigma_\mu$, $\alpha_{x,y} = \sigma_x^+\sigma_y + \sigma_y^+\sigma_x$, and σ_k denotes the expression (40) for $m = n$. In the isotropic case, Eq. (53) becomes just $4\sigma(2\sigma^+ - \sigma)\cos^2\frac{\pi k}{n}$. For the parallel and tilted subsystems of Figs. 3(c) and 3(d) we then obtain, replacing sums by integrals and assuming $\sigma \leqslant 2\sigma^+$,

$$\tilde{\mathcal{E}}^{\mathcal{N}c}_{\mathcal{B},\bar{\mathcal{C}}} \approx n\sigma(2\sigma^+ - \sigma), \tag{54a}$$

$$\tilde{\mathcal{E}}^{\mathcal{N}d}_{\mathcal{B},\bar{\mathcal{C}}} \approx 2n\sigma(2\sigma^+ - \sigma). \tag{54b}$$

Hence, the logarithmic negativity of the tilted case is, remarkably, *twice* that of parallel blocks when separated by one site, instead of $4/\pi \approx 1.27$ as in the contiguous case (Fig. 4). Since they are a second-order effect, Eqs. (54) are not of the form (45)

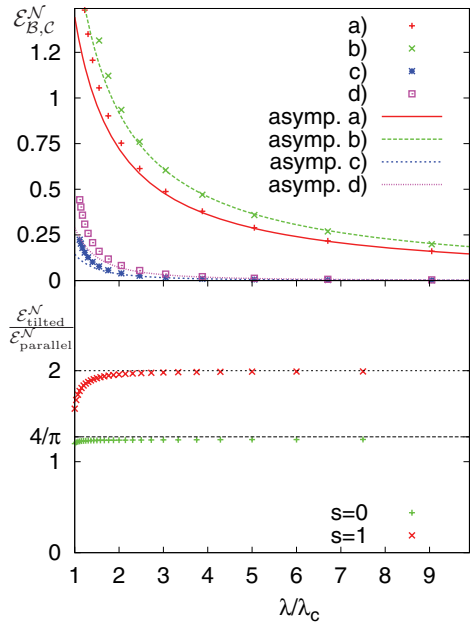

FIG. 4. (Color online) Top: Exact and asymptotic logarithmic negativities [Eqs. (50) and (51)] for subsystems of the type of Fig. 3 (for 10×10 blocks) as functions of λ/λ_c. Tilted blocks exhibit a larger negativity per contacting site. Bottom: The ratio of tilted to parallel logarithmic negativities for separations $s = 0$ (a),(b) and 1 (c),(d). It is asymptotically $4/\pi$ in the contiguous case and 2 for one-site separation.

but rather

$$\tilde{\mathcal{E}}^{\mathcal{N}}_{\mathcal{B},\bar{\mathcal{C}}} \approx Lm\sigma(2\sigma^{+} - \sigma), \tag{55}$$

if m is again the number of connections with the environment per mode. They scale, therefore, with the measure $|\partial\mathcal{A}|_2$ (Fig. 5). For larger separations s the negativity vanishes at second order in Δ/λ, as $F^{-}_{\mathcal{B},\mathcal{C}}$ will be of higher order while the counterterms $G_{\mathcal{B}}$ and $G_{\mathcal{C}}$ remain of second order for sites at the surface. Consequently, the negativity becomes vanishingly small for $s \geqslant 2$.

We finally remark that previous expressions are independent (at leading order) of the width d of the blocks (assumed finite), *provided* $d \geqslant 2$. In the case of two lines ($d = 1$, Fig. 6), the extra interaction with the environment at the other side of the line leads to an additional negative second-order contribution in Eq. (26). Hence, while it can be neglected in the case of contiguous lines, it will double the negative term in Eqs. (54) in the case of lines separated by one site, leading to the lower values

$$\tilde{\mathcal{E}}^{\mathcal{N}e}_{\mathcal{B},\bar{\mathcal{C}}} \approx n\sigma(2\sigma^{+} - 2\sigma), \tag{56a}$$

$$\tilde{\mathcal{E}}^{\mathcal{N}f}_{\mathcal{B},\bar{\mathcal{C}}} \approx 2n\sigma(2\sigma^{+} - 2\sigma), \tag{56b}$$

which are now valid for $\sigma \leqslant \sigma^{+}$. In this case the negativity will vanish at second order if $\sigma > \sigma^{+}$. Edge effects in Eqs. (54)–(56) are also of second order and lead, using Eq. (25), to a negative correction $-2\sigma^2$.

All present expressions can be directly extended to three dimensions if the present subsystems are extended parallelwise along the z axis, replacing n by nn_z.

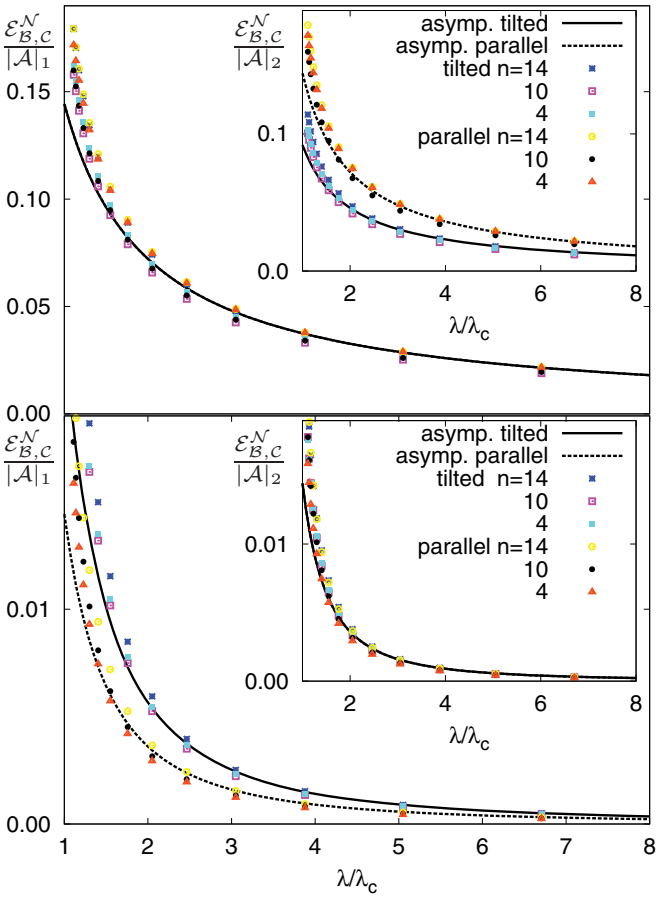

FIG. 5. (Color online) Top: Asymptotic and exact values of the logarithmic negativity of two contiguous $n \times n$ blocks with parallel and tilted boundary surfaces, scaled with $|\partial\mathcal{A}|_1$ in the main panel and $|\partial\mathcal{A}|_2$ in the inset, with $\partial\mathcal{A} = \partial\mathcal{B} \cap \partial\mathcal{C}$. Bottom: Same details for two blocks separated by one site. The appropriate scaling is verified to be $|\partial\mathcal{A}|_1$ in the top panel and $|\partial\mathcal{A}|_2$ in the bottom panel.

C. The fully connected case

The evaluation of singular values is also straightforward in the opposite case of a fully and uniformly connected system of n modes [24,30–32] (Lipkin-Meshkov-Glick (LMG)-type model [23]), where

$$\Delta^{\pm}_{ij} = (1 - \delta_{ij})\frac{\Delta^{\pm}}{n-1}. \tag{57}$$

Here we can also compare with the full exact results, since it is exactly and analytically solvable [24,31]. The present system can be used to describe entanglement between systems whose separation is small in comparison with the correlation length.

In the present case, the matrices $F^{\pm}_{ij}$ are obviously constant for $i \neq j$, i.e.,

$$F^{\pm}_{ij} = F^{\pm}_{0}\delta_{ij} + F^{\pm}_{1}, \tag{58}$$

and the entanglement between disjoint subsystems $\mathcal{B}$ and $\mathcal{C}$ will just depend on the number of sites in $\mathcal{B}$ and in $\mathcal{C}$, being independent of their separation or shape. The matrix $F^{-}_{\mathcal{B},\mathcal{C}}$ will then have just a *single* nonzero singular value, for all disjoint $\mathcal{B}$,$\mathcal{C}$, namely (see Appendix C),

$$\sigma^{\mathcal{B},\mathcal{C}} = \sqrt{n_{\mathcal{B}}n_{\mathcal{C}}}|F^{-}_{1}|. \tag{59}$$

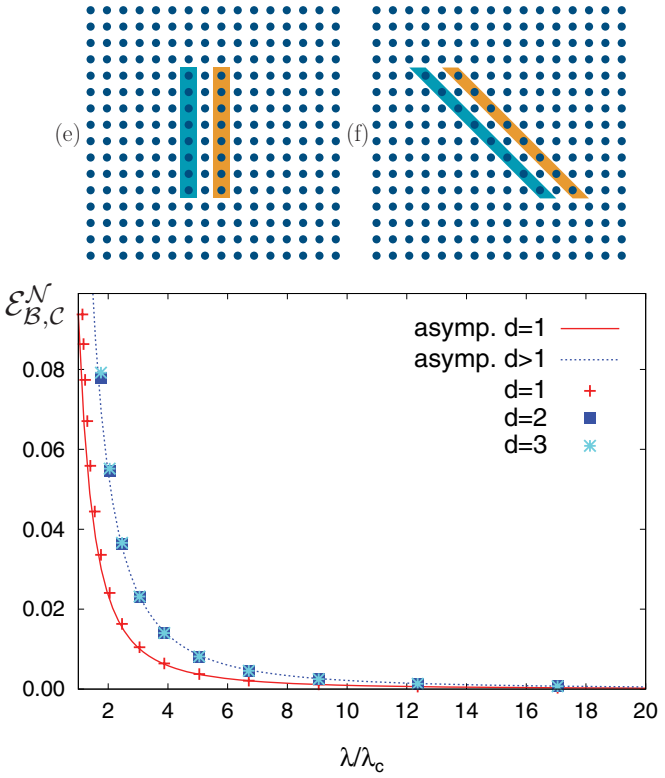

FIG. 6. (Color online) Top: Parallel and tilted lines separated by one site. Due to the extra interaction with the environment, the associated negativity [Eqs. (56)] is lower than that of the corresponding blocks of Figs. 3(c) and 3(d) [Eqs. (54)], as can be seen in the bottom panels for the parallel case.

In the approximation (19) we then obtain a single nonzero symplectic eigenvalue for any global bipartition $\mathcal{A},\bar{\mathcal{A}}$,

$$f^{\mathcal{A}} \approx n_{\mathcal{A}} n_{\bar{\mathcal{A}}} (F_1^-)^2, \tag{60}$$

where $n_{\bar{\mathcal{A}}} = n - n_{\mathcal{A}}$, leading to

$$\mathcal{E}_{\mathcal{A},\bar{\mathcal{A}}} \approx -n_{\mathcal{A}} n_{\bar{\mathcal{A}}} |F_1^-|^2 \log_2[n_{\mathcal{A}} n_{\bar{\mathcal{A}}} (F_1^-)^2/e],$$

which corresponds to an area $|\partial\mathcal{A}|_2 = n_{\mathcal{A}} n_{\bar{\mathcal{A}}}$ in Eq. (32) (here $M_{ij} = 1$ for $i \neq j$).

Similarly, we obtain a single negative symplectic eigenvalue for any pair of subsystems $\mathcal{B},\mathcal{C}$, given by Eq. (59) or, in the complete approximation (21)–(25), by

$$\tilde{f}^{\mathcal{B},\mathcal{C}} \approx -\sqrt{n_{\mathcal{B}} n_{\mathcal{C}}} |F_1^-| + \tfrac{1}{2} |F_1^-|^2 (n_{\mathcal{B}} n_{\bar{\mathcal{B}}} + n_{\mathcal{C}} n_{\bar{\mathcal{C}}}), \tag{61}$$

with $\mathcal{E}^{\mathcal{N}}_{\mathcal{B},\mathcal{C}} = -\tilde{f}_{\mathcal{B},\mathcal{C}}$. The second term in Eq. (61) becomes important for small subsystems in a large environment ($n_{\mathcal{B}}, n_{\mathcal{C}} \ll n$). Otherwise it can be neglected, in which case (61) corresponds to $|\partial\mathcal{A}|_1 = \sqrt{n_{\mathcal{B}} n_{\mathcal{C}}}$ in Eqs. (33)–(36). For the scaling (57), F_1^- is proportional to n^{-1}, so that Eqs. (59)–(61) remain finite for large n. The scaling is then again as in Eqs. (44) and (45) with $L = 1$, $j = 0$, and $m = n_{\mathcal{A}} n_{\bar{\mathcal{A}}}$ for global partitions or $m = n_{\mathcal{B}} n_{\mathcal{C}}$ for a pair of subsystems.

The previous picture is, remarkably, also that of the exact treatment, where there is a single nonzero symplectic eigenvalue $f^{\mathcal{A}}$ for any subsystem $\mathcal{A}$, given by

$$f^{\mathcal{A}} = \sqrt{\frac{1}{4} + F_1^+ n_{\mathcal{A}} n_{\bar{\mathcal{A}}}/n} - \frac{1}{2}, \tag{62}$$

(see Ref. [24] and Appendix C). Here we have used the local basis where $F_0^{\pm} = 0$ in Eq. (57), in which case Eq. (7) leads to

$$F_1^{+2} + F_1^+/n = (F_1^-)^2.$$

A first-order expansion of Eq. (62) in F_1^+ leads then to $f^{\mathcal{A}} \approx F_1^+ n_{\mathcal{A}} n_{\bar{\mathcal{A}}}/n$, which coincides with Eq. (60) since for weak coupling $F_1^+/n \approx (F_1^-)^2$.

In the same way, the exact partial transpose of $\mathcal{D}_{\mathcal{BC}}$ has a single negative symplectic eigenvalue [24]

$$\tilde{f}^{\mathcal{B},\mathcal{C}} = \sqrt{\frac{1}{4} + \gamma_{\mathcal{B},\mathcal{C}} F_1^+ - \sqrt{F_1^+ \left(\beta_{\mathcal{B},\mathcal{C}} + \gamma_{\mathcal{B},\mathcal{C}}^2 F_1^+\right)}} - \frac{1}{2}, \tag{63}$$

where $\beta_{\mathcal{B},\mathcal{C}} = n_{\mathcal{B}} n_{\mathcal{C}}/n$ and $\gamma_{\mathcal{B},\mathcal{C}} = \frac{1}{2}(n_{\mathcal{B}} + n_{\mathcal{C}})(n - n_{\mathcal{B}} - n_{\mathcal{C}})/n + 2\beta_{\mathcal{B},\mathcal{C}}$ (see Appendix C). Expansion of Eq. (63) up to first order in F_1^+ leads then exactly to Eq. (61), setting $F_1^+ \approx n(F_1^-)^2$. The present approximate scheme then allows one to immediately determine the weak-coupling expressions (60) and (61) and to rapidly identify their behavior with sizes $n_{\mathcal{A}}, n_{\mathcal{B}}, n_{\mathcal{C}}$. The exact value of $F_1^{\pm}$ [to be inserted in Eqs. (62) and (63)] is given in Appendix C [Eq. (C4)]. Up to first order in Δ_- we obtain $F_1^- \approx \frac{\Delta^-}{2(n-1)\lambda}$.

IV. CONCLUSIONS

We have shown how entanglement properties of weakly correlated Gaussian states can be recast in terms of the singular values of a sub-block of the generalized contraction matrix associated with the state. This allows us to obtain in a quite simple way analytic expressions for both the entanglement entropy between complementary subsystems and the logarithmic negativity for noncomplementary subsystems, which imply distinct area laws for these two quantities in the case of short-range or constant couplings. Several illustrative examples were considered, which show the dependence of these laws on the geometry, connectivity, and separation between the subsystems. A final comment is that through application of the bosonic random-phase approximation formalism [24,29,33] or other bosonization treatments [23,31], the present scheme can be applied to weakly interacting spin systems. Moreover, it can in principle also be implemented in phases exhibiting symmetry breaking at the mean-field level (i.e., fields below the critical field in attractive XY or XYZ chains) away from the critical field, provided the proper multiplicity corrections accounting for the different degenerate mean fields [24] are taken into account. Such an application is currently being investigated.

ACKNOWLEDGMENTS

The authors acknowledge the support of CONICET (N.C., J.M.M.) and CIC (R.R.) of Argentina.

APPENDIX A: PERTURBATIVE EXPANSIONS FOR THE SYMPLECTIC EIGENVALUE PROBLEM

In this work we have used perturbative results which are not necessarily trivial and which can be obtained following techniques similar to those employed in the perturbative diagonalization of the Dirac equation. We start with the

symplectic diagonalization of the contraction matrix $\mathcal{D}_\mathcal{A}$ of a subsystem $\mathcal{A}$, which leads to the system

$$F^+_\mathcal{A} U_f - F^-_\mathcal{A} V_f = f U_f, \tag{A1}$$
$$\bar{F}^-_\mathcal{A} U_f - (\mathbf{1} + \bar{F}^+_\mathcal{A})\bar{V}_f = f \bar{V}_f, \tag{A2}$$

where $\binom{U_f}{\bar{V}_f}$ is the symplectic eigenvector associated with the eigenvalue f. Equation (A2) allows us to write V_f as

$$\bar{V}_f = [\mathbf{1}(1+f) + \bar{F}^+_\mathcal{A}]^{-1} \bar{F}^-_\mathcal{A} U_f. \tag{A3}$$

Replacing (A3) in Eq. (A1) leads to the equivalent nonlinear reduced diagonalization problem

$$\{F^+_\mathcal{A} - F^-_\mathcal{A}[\mathbf{1}(1+f) + \bar{F}^+_\mathcal{A}]^{-1} \bar{F}^-_\mathcal{A}\} U_f = f U_f.$$

For small $F^\pm$, in agreement with the hypothesis that the state is weakly correlated, the symplectic eigenvalues f are small. Hence, at leading order $\bar{V}_f \approx \bar{F}^-_\mathcal{A} U_f$ and we obtain the reduced standard eigenvalue equation

$$(F^+_\mathcal{A} - F^-_\mathcal{A} \bar{F}^-_\mathcal{A}) U_f = f U_f, \tag{A4}$$

which leads to Eq. (18) and implies Eq. (21). If $\mathcal{A}$ is the whole system and the latter is assumed to be in the ground state of H, all f vanish and the relation $F^+ \approx F^- \bar{F}^-$ [Eq. (16)] is obtained.

Let us now consider the Hamiltonian (2). The symplectic diagonalization of $\mathcal{H}$ entails the standard diagonalization of $\mathcal{M}\mathcal{H}$ and leads to the system

$$(\Lambda - \Delta^+) U_\omega - \Delta^- \bar{V}_\omega = \omega U_\omega, \tag{A5}$$
$$\bar{\Delta}^- U_\omega - (\Lambda - \bar{\Delta}^+) \bar{V}_\omega = \omega \bar{V}_\omega. \tag{A6}$$

In this case, $\|\Delta^-\|_\infty$ is considered small. For a positive eigenvalue, the zero-order approximation is obtained by neglecting all terms proportional to Δ^- and $\bar{V}_\omega$, which are assumed small in comparison with U_ω, ω, and $\Lambda - \Delta^+$. It leads to $(\Lambda - \Delta^+) U_\omega = \omega U_\omega$, which is a standard Hermitian eigenvalue equation for U_ω. We then obtain

$$\bar{V}_\omega = (\Lambda - \bar{\Delta}^+ + \omega \mathbf{1})^{-1} \bar{\Delta}^- U_\omega \tag{A7}$$
$$\approx U^* (\Omega + \omega \mathbf{1})^{-1} U^t \bar{\Delta}^- U_\omega \tag{A8}$$

[Eq. (28)], where we have written $\Lambda - \Delta^+ \approx U \Omega U^\dagger$, with $\Omega = \mathrm{diag}(\omega_\alpha)$ the diagonal matrix of eigenvalues. It should be noticed that if Λ is degenerate, Δ^+ will affect U considerably even if small. Ground-state entanglement will remain small, however, since it depends on V. It can also be easily seen that expansion of Eq. (A7) up to second order in $\Delta^\pm$ leads to Eq. (30).

APPENDIX B: SINGULAR VALUES

The singular values σ_α of an arbitrary $m \times n$ matrix A are the square roots of the nonzero eigenvalues of $AA^\dagger$ or equivalently $A^\dagger A$, which are both positive matrices with the same nonzero eigenvalues. The singular value decomposition implies the existence of unitary matrices U,V such that $A = UDV^\dagger$, with D a diagonal matrix with diagonal elements σ_α or 0, and U,V unitary eigenvector matrices of $AA^\dagger$ and $A^\dagger A$: $AA^\dagger U = UDD^\dagger$, $A^\dagger A V = V D^\dagger D$, i.e., $AA^\dagger U_\alpha = \sigma_\alpha^2 U_\alpha$, $A^\dagger A V_\alpha = \sigma_\alpha^2 V_\alpha$ for the nonzero eigenvalues σ_α, with $V_\alpha = A^\dagger U_\alpha / \sigma_\alpha$. For a Hermitian A, $\sigma_\alpha = |\lambda_\alpha|$, with λ_α the (nonzero) eigenvalues of A.

The singular values determine the matrix m norm of A used in this work, defined as

$$\|A\|_m = [\mathrm{Tr}(A^\dagger A)^{m/2}]^{1/m} = \left(\sum_\alpha \sigma_\alpha^m \right)^{1/m}. \tag{B1}$$

$\|A\|_1$ is the trace norm, $\|A\|_2$ the standard Hilbert-Schmidt norm, and $\|A\|_\infty$ the spectral norm, which is just the largest singular value.

The singular values σ_α of A also determine the nonzero eigenvalues of the Hermitian $(m+n) \times (m+n)$ matrix

$$B = \begin{pmatrix} 0 & A \\ A^\dagger & 0 \end{pmatrix}, \tag{B2}$$

which are $\pm\sigma_\alpha$, since $B^2 = \left(\begin{smallmatrix} AA^\dagger & 0 \\ 0 & A^\dagger A \end{smallmatrix}\right)$ has eigenvalues σ_α^2. The eigenvalues $\pm\sigma_\alpha$ correspond to normalized eigenvectors $\binom{U_\alpha}{\pm V_\alpha}/\sqrt{2}$, with $AA^\dagger U_\alpha = \sigma_\alpha^2 U_\alpha$, $V_\alpha = A^\dagger U_\alpha / \sigma_\alpha$ and $U_\alpha^\dagger U_\beta = \delta_{\alpha\beta}$, $V_\alpha^\dagger V_\beta = \delta_{\alpha\beta}$.

These results first imply that the nonzero eigenvalues of the matrix (18) are the squares of the singular values $\sigma_\alpha^{\mathcal{A},\bar{\mathcal{A}}}$ of $F^-_{\mathcal{A},\bar{\mathcal{A}}}$, as $\bar{F}^-_{\bar{\mathcal{A}},\mathcal{A}} = (F^-_{\mathcal{A},\bar{\mathcal{A}}})^\dagger$, implying $\sigma_\alpha^{\mathcal{A},\bar{\mathcal{A}}} = \sigma_\alpha^{\bar{\mathcal{A}},\mathcal{A}}$. They also entail that the negative eigenvalues of the matrix (21) are minus the singular values $\sigma_\alpha^{\mathcal{B},\mathcal{C}} = \sigma_\alpha^{\mathcal{C},\mathcal{B}}$ of $F^-_{\mathcal{B},\mathcal{C}}$, when $\bar{G}_\mathcal{B}$ and $G_\mathcal{C}$ are neglected.

APPENDIX C: EVALUATION OF SINGULAR VALUES

In the first-order approximation (29), the matrix $F^-_{\mathcal{B},\mathcal{C}}$ for first-neighbor couplings and disjoint contiguous blocks $\mathcal{B}$ and $\mathcal{C}$ with n contacting sites has elements of the form

$$(F^-_{\mathcal{B},\mathcal{C}})_{ij} = f(j-i) \tag{C1}$$

if the sites are adequately ordered, where $f(l) = \delta_{l0} \sigma_{\mu\perp}$ for parallel and $f(l) = \sigma_x \delta_{l0} + \sigma_y \delta_{l1}$ for tilted blocks.

For blocks separated by one site, we should use the second-order approximation (30), which leads again to a matrix of the form (C1), with $f(l) = 2\delta_{l0} \sigma^+ \sigma$ for parallel blocks and $f(l) = 2[\sigma_x^+ \sigma_x \delta_{l0} + (\sigma_x^+ \sigma_y + \sigma_y^+ \sigma_x)\delta_{l1} + \sigma_y^+ \sigma_y \delta_{l2}]$ for tilted blocks. In all previous cases, $F^-_{\mathcal{B},\mathcal{C}} \bar{F}^-_{\mathcal{C},\mathcal{B}}$ is a Hermitian matrix with elements of the form

$$(F^-_{\mathcal{B},\mathcal{C}} \bar{F}^-_{\mathcal{C},\mathcal{B}})_{ij} = \sum_k f(k-i) \bar{f}(k-j) = g(i-j), \tag{C2}$$

if edge effects are neglected, where $g(l) = \sum_k f(k) \bar{f}(k+l) = \bar{g}(-l)$. Such a matrix can then be exactly diagonalized (neglecting edge effects) by a discrete Fourier transform [32], leading to eigenvalues $\sigma_k^2 = \sum_l g(l) e^{i 2\pi k l / n}$, where $k = 0, \ldots, n-1$ and n is its dimension [this result is exact if $g(-l) = g(n-l)$]. For real $g(l)$, as in the previous cases, we then obtain

$$\sigma_k^2 = g(0) + 2 \sum_{l>0} g(l) \cos \frac{2\pi k}{n}, \tag{C3}$$

which leads to Eqs. (40)–(53) [in the case of $\mathcal{C} = \bar{\mathcal{A}}$ with $\mathcal{A}$ the tilted block, the final matrix $F^-_{\mathcal{A},\bar{\mathcal{A}}} \bar{F}^-_{\bar{\mathcal{A}},\mathcal{A}}$ is again of the form (C2)].

In the fully connected case, the exact singular values (59) arise immediately as the matrix $F^-_{\mathcal{B},\mathcal{C}}$ is just a rank-1 constant

matrix, i.e., $F^-_{\mathcal{B},\mathcal{C}} = c$, $\forall\ i,j$, which therefore has a unique nonzero singular value $\sigma = \sqrt{n_{\mathcal{B}} n_{\mathcal{C}}}|c|$: $F^-_{\mathcal{B},\mathcal{C}} \bar{F}^-_{\mathcal{C},\mathcal{B}}$ is an $n_{\mathcal{B}} \times n_{\mathcal{B}}$ rank-1 matrix with constant elements $n_{\mathcal{C}}|c|^2$, whose unique nonzero eigenvalue is $n_{\mathcal{B}} n_{\mathcal{C}}|c|^2$ due to trace conservation.

The full exact symplectic diagonalization can also be performed (see the Appendix in Ref. [24] for details). We quote here the exact symplectic eigenvalues of the reduced state of L sites for the couplings (57): $\sigma_1 = \sqrt{(F_0^+ + LF_1^+ + \frac{1}{2})^2 - (F_0^- + LF_1^-)^2} - \frac{1}{2}$ and $\sigma_0 = \sqrt{(F_0^+ + \frac{1}{2})^2 - (F_0^-)^2} - \frac{1}{2}$ [$(L-1)$-fold degenerate]. For a pure global state, $\sigma_0 = 0$. In the local basis where $F_0^- = 0$, this implies $F_0^+ = 0$, which leads to Eq. (62). In the same way, we obtain Eq. (63). The exact value of the present F_1^+ was also evaluated in Ref. [24] in terms of a parameter Δ [$F_1^+ = \Delta/(2n)$]:

$$F_1^+ = \frac{n(\lambda^2 - \bar{\omega}^2)}{4(n-1)\omega_0\omega_1}, \tag{C4}$$

where $\bar{\omega} = \frac{\omega_0 + (n-1)\omega_1}{n}$, $\omega_0 = \sqrt{(\lambda - \Delta_x)(\lambda - \Delta_y)}$, and $\omega_1 = \sqrt{(\lambda + \frac{\Delta_x}{n-1})(\lambda + \frac{\Delta_y}{n-1})}$, with $\Delta_\pm = (\Delta_x \pm \Delta_y)/2$.

[1] M. A. Nielsen and I. L. Chuang, *Quantum Computation and Quantum Information* (Cambridge University Press, Cambridge, UK, 2000).

[2] C. H. Bennett, G. Brassard, C. Crepeau, R. Jozsa, A. Peres, and W. K. Wootters, Phys. Rev. Lett. **70**, 1895 (1993).

[3] R. Josza and N. Linden, Proc. R. Soc. London, A **459**, 2011 (2003); G. Vidal, Phys. Rev. Lett. **91**, 147902 (2003).

[4] R. Raussendorf and H. J. Briegel, Phys. Rev. Lett. **86**, 5188 (2001); R. Raussendorf, D. E. Browne, and H. J. Briegel, Phys. Rev. A **68**, 022312 (2003).

[5] C. Weedbrook *et al.*, Rev. Mod. Phys. **84**, 621 (2012).

[6] A. Osterloh, L. Amico, G. Falci, and R. Fazio, Nature (London) **416**, 608 (2002).

[7] T. J. Osborne and M. A. Nielsen, Phys. Rev. A **66**, 032110 (2002).

[8] G. Vidal, J. I. Latorre, E. Rico, and A. Kitaev, Phys. Rev. Lett. **90**, 227902 (2003).

[9] L. Amico, R. Fazio, A. Osterloh, and V. Vedral, Rev. Mod. Phys. **80**, 517 (2008).

[10] J. Eisert, M. Cramer, and M. B. Plenio, Rev. Mod. Phys. **82**, 277 (2010).

[11] C. H. Bennett, H. J. Bernstein, S. Popescu, and B. Schumacher, Phys. Rev. A **53**, 2046 (1996).

[12] C. H. Bennett, D. P. DiVincenzo, J. A. Smolin, and W. K. Wootters, Phys. Rev. A **54**, 3824 (1996).

[13] P. Rungta and C. M. Caves, Phys. Rev. A **67**, 012307 (2003); P. Rungta, V. Bužek, C. M. Caves, M. Hillery, and G. J. Milburn, *ibid.* **64**, 042315 (2001).

[14] G. Vidal and R. F. Werner, Phys. Rev. A **65**, 032314 (2002).

[15] M. B. Plenio, Phys. Rev. Lett. **95**, 090503 (2005).

[16] A. S. Holevo, M. Sohma, and O. Hirota, Phys. Rev. A **59**, 1820 (1999).

[17] R. Simon, Phys. Rev. Lett. **84**, 2726 (2000).

[18] K. Audenaert, J. Eisert, M. B. Plenio, and R. F. Werner, Phys. Rev. A **66**, 042327 (2002).

[19] M. B. Plenio, J. Eisert, J. Dreißig, and M. Cramer, Phys. Rev. Lett. **94**, 060503 (2005); M. Cramer, J. Eisert, M. B. Plenio, and J. Dreißig, Phys. Rev. A **73**, 012309 (2006).

[20] M. Cramer, J. Eisert, and M. B. Plenio, Phys. Rev. Lett. **98**, 220603 (2007).

[21] G. Adesso, A. Serafini, and F. Illuminati, Phys. Rev. Lett. **93**, 220504 (2004); Phys. Rev. A **70**, 022318 (2004); A. Serafini, G. Adesso, and F. Illuminati, *ibid.* **71**, 032349 (2005).

[22] G. Adesso and F. Illuminati, Phys. Rev. A **78**, 042310 (2008).

[23] P. Ring and P. Schuck, *The Nuclear Many-Body Problem* (Springer, New York, 1980).

[24] J. M. Matera, R. Rossignoli, and N. Canosa, Phys. Rev. A **82**, 052332 (2010).

[25] S. Marcovitch, A. Retzker, M. B. Plenio, and B. Reznik, Phys. Rev. A **80**, 012325 (2009).

[26] P. Calabrese and J. Cardy, J. Stat. Mech.: Theory Exp. (2004) P06002.

[27] V. E. Korepin, Phys. Rev. Lett. **92**, 096402 (2004); B.-Q. Jin and V. E. Korepin, J. Stat. Phys. **116**, 79 (2004).

[28] J. I. Latorre, R. Orús, E. Rico, and J. Vidal, Phys. Rev. A **71**, 064101 (2005).

[29] R. Rossignoli, N. Canosa, and J. M. Matera, Phys. Rev. A **83**, 042328 (2011).

[30] T. Barthel, S. Dusuel, and J. Vidal, Phys. Rev. Lett. **97**, 220402 (2006); J. Vidal, S. Dusuel, and T. Barthel, J. Stat. Mech.: Theory Exp. (2007) P01015.

[31] H. Wichterich, J. Vidal, and S. Bose, Phys. Rev. A **81**, 032311 (2010).

[32] J. M. Matera, R. Rossignoli, and N. Canosa, Phys. Rev. A **78**, 012316 (2008).

[33] J. M. Matera, R. Rossignoli, and N. Canosa, Phys. Rev. A **78**, 042319 (2008).